Transformations of Manool. Tri- and Tetracyclic Norditerpenoids with *in Vitro* Activity against *Plasmodium falciparum*

Albert W. W. van Wyk,[†] Kevin A. Lobb,[†] Mino R. Caira,[‡] Heinrich C. Hoppe,[§] and Michael T. Davies-Coleman*[,†]

Department of Chemistry, Rhodes University, Grahamstown, South Africa, Department of Chemistry, University of Cape Town, Rondebosch, South Africa, and Division of Pharmacology, Faculty of Health Sciences, University of Cape Town, Observatory, South Africa

Received March 12, 2007

The known 17-norisopimar-15-ene-8β,13β-diol (**5**) and five new semisynthetic norditerpenoids, ethyl 17-norabiet-13-(15)-*E*-en-8β-ol-16-oate (**6**), ethyl 17-norabiet-13(15)-*Z*-en-8β-ol-16-oate (**7**), 17-norpimaran-13α-ethoxy-8,16-olactone (**8**), 17-norisopimarane-8β,15-diol (**9**), and 17-norarabiet-13(15)-ene-8β,16-diol (**10**), were prepared from manool (**11**). Standard spectroscopic data including X-ray crystal analysis were used to determine the structures of **5**−**10**. All five compounds exhibited *in vitro* antiplasmodial activity against the malarial parasite *Plasmodium falciparum* at varying μg mL^{-1} concentrations.

Malaria affects 300−660 million individuals per annum worldwide and results in an estimated 1−2 million deaths, mostly in children under the age of 5.[1] More than 70% of the malaria cases and deaths occur in sub-Saharan Africa, where the disease has a crippling impact on the already fragile socioeconomic and public health structures of some of the world's poorest nations.[2] The erythrocytic stages of the malarial protozoan parasites of the genus *Plasmodium*, predominantly *P. falciparum*, are readily cultured *in vitro* and continue to provide a target for the renewed and urgent antimalarial drug discovery efforts prompted by the alarming and widespread occurrence of parasite resistance to the foremost antimalarial drugs, notably chloroquine and sulfadoxine-pyrimethamine.[3]

Terrestrial plants have historically been a vital source of antimalarials, with quinine from the South American *Cinchona* tree, from which chloroquine and related quinolines were derived, and artemesinin and its derivatives from the Chinese herb *Artemisia annua*, currently among the most promising antimalarials.[4,5] The disappointing rate at which synthetic chemical libraries and defined molecular target-based drug discovery programs are perceived to be delivering new drugs has renewed interest in natural products as a potential source of novel antimalarial compounds.[6,7] Recently a series of isopimarane diterpenoids (**1**−**4**) with antiplasmodial activity (IC_{50} 7−25 μg mL^{-1}) and reportedly hemolytic properties were isolated from the Iranian tree *Platycladus orientalis* (L.) Franco (Cupressaceae).[8] In order to explore the possibility of improved antiplasmodial activity and reduced hemolytic properties in compounds possessing either norisopimarene, norabietene, or norpimarane as opposed to an isopimarane skeleton, we have prepared a cohort of six 17-norditerpenoids (**5**−**10**), related to **1**−**4**, from the naturally occurring labdane diterpenoid (+)-manool (**11**). The semisyntheses and antiplasmodial and hemolytic properties of **5**−**10** are reported here.

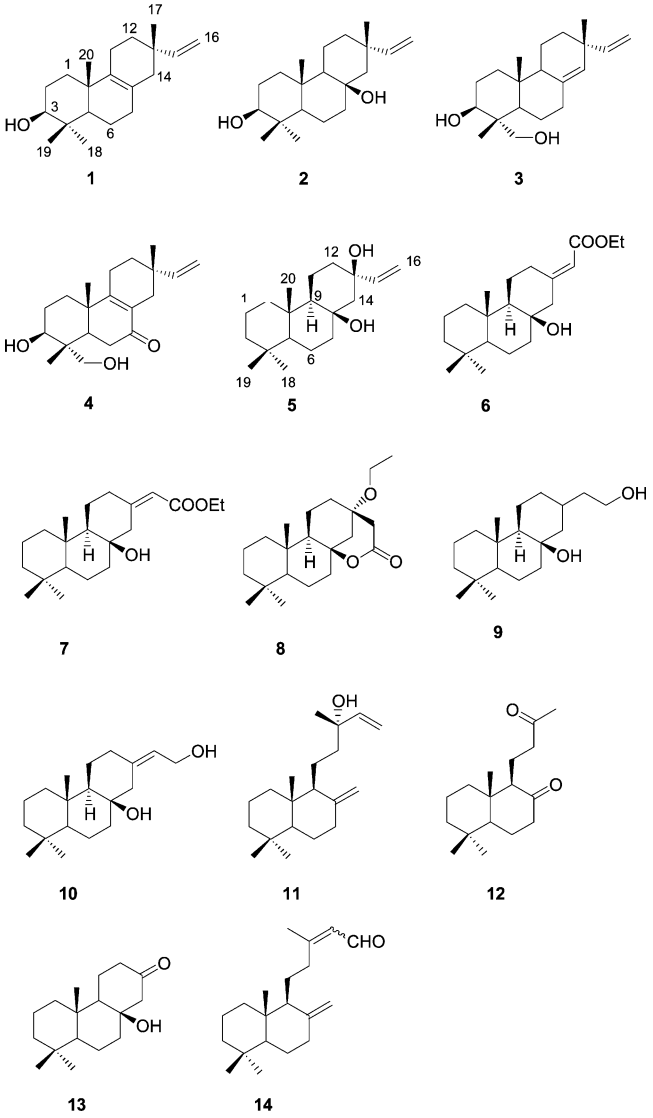

Results and Discussion

(+)-Manool is regularly used as a semisynthetic precursor in the syntheses of both marine and terrestrial natural products,[9−11] and our initial target, **5**, was also originally synthesized from this compound.[12] Wenkert and co-workers' semisynthesis of **5** incorporated an initial intramolecular aldol condensation of the diketone (**12**) followed by nucleophilic addition of vinyl magnesium bromide to the resultant 8-hydroxy-13-podocarpanone (**13**).[12] The apparent *si*-facial selectivity of the Grignard reaction was corroborated by absorbances consistent with a *cis* 1,3-diol in the IR spectrum of **5**.[12] Diketone **12** has been previously accessed in 72% and 36% overall yield, respectively, from **11** via oxidation of this compound with either a combination of OsO_4/HIO_5 at pH 6 or $KMnO_4$ and

* To whom correspondence should be addressed. Tel: +27 46 603 8294. Fax: +27 46 6225109. E-mail: M.Davies-Coleman@ru.ac.za.
[†] Rhodes University.
[‡] Department of Chemistry, University of Cape Town.
[§] Division of Pharmacology, University of Cape Town.

10.1021/np0701071 CCC: $37.00
Published on Web 07/11/2007

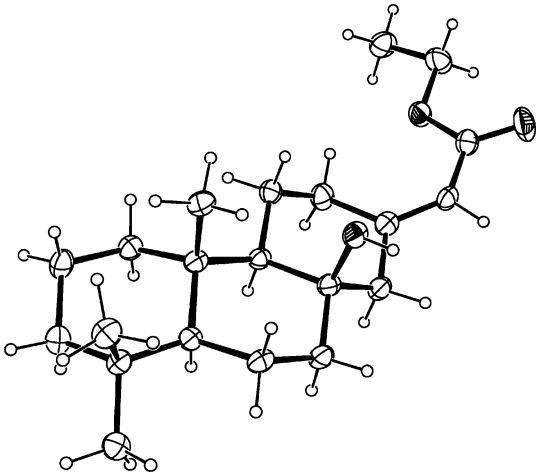

Figure 1. View of a molecule of ethyl 17-norabiet-13(15)-*E*-en-8*β*-ol-16-oate (**6**) from the crystal structure. Thermal ellipsoids for the non-hydrogen atoms are shown at the 50% probability level.

subsequent ozonolysis.[12−14] We, however, elected to modify our preliminary synthesis of **12** from **11** using an initial high-yielding pyridinium chlorochromate mediated oxidative rearrangement of **11**[15] to give a 2:1 mixture of the *E* and *Z* isomers (as determined from NMR analysis) of the α,*β*-unsaturated aldehyde (**14**). Reductive ozonolysis of *E*/*Z*-**14** afforded **12** in an overall yield (71%) from **11** comparable with reported yields.[12−14]

With **12** in hand we performed an NaH-mediated intramolecular aldol condensation to access **13** in quantitative yield, which was a significant improvement in the yields reported for the intramolecular aldol condensation of **12** induced by methanolic KOH (68%)[12] and ethanolic NaOEt (80%).[14] The apparent instability of **13** required prompt reaction of this aldol condensation product with vinyl magnesium bromide under standard Grignard conditions. Silica chromatography of the reaction mixture gave the desired 17-norisopimarene-8,13-diol product **5** in 24% overall yield from **11**. Regrettably, Wenkert and co-workers[12] did not report the specific rotation of **5** and provided only a melting point and ^{13}C NMR data for this compound. Comparison of melting point and ^{13}C NMR data obtained for our synthetic product with published data for **5**[12] confirmed the structure of our compound.

The synthesis of **5** highlighted the suitability of the C-13 ketone moiety in **13** as a key to further structural elaboration. Accordingly, the ketone functionality in **13** was converted into a trisubstituted olefin using a Horner−Wadsworth−Emmons (HWE) modification of the Wittig reaction.[16] The stereoselectivity of the HWE reaction is diminished when ketones are used to prepare trisubstituted alkenes,[17] and reaction of **13** with triethylphosphonoacetate under standard HWE conditions (NaH and anhydrous THF) gave a 4:3 ratio of ethyl 17-norabiet-13(15)-*E*-en-8*β*-ol-16-oate (**6**) and ethyl 17-norabiet-13(15)-*Z*-en-8*β*-ol-16-oate (**7**) in 70% yield. These two compounds were assigned to the norabietane diterpenoid series as opposed to the norpimarane or norisopimarane series because the C_2 substitutent at C-13 (i.e., the $\Delta^{13(15)}$ olefin) in **6** and **7** has neither a *syn* nor an *anti* relationship with the angular methyl group at C-10 required for membership to either the pimarane or isopimarane series, respectively.[18] The two isomers were readily separated by normal-phase HPLC (9:1 hexane/EtOAc). Crystals of **6**, obtained by slow crystallization from Et_2O/hexane, were deemed suitable for X-ray analysis, and a perspective view of the molecular structure of this compound is presented in Figure 1.[19]

The instability of **13** coupled with the use of NaH in anhydrous THF for both the intramolecular aldol condensation and the HWE reaction encouraged us to investigate a one-pot synthesis of **6** and **7** from the diketone **12**. Thus, **12** was first stirred with NaH (2.6 equiv) in dry THF (4 h) before dropwise addition of a solution of deprotonated triethylphosphonacetate HWE reagent. Although this

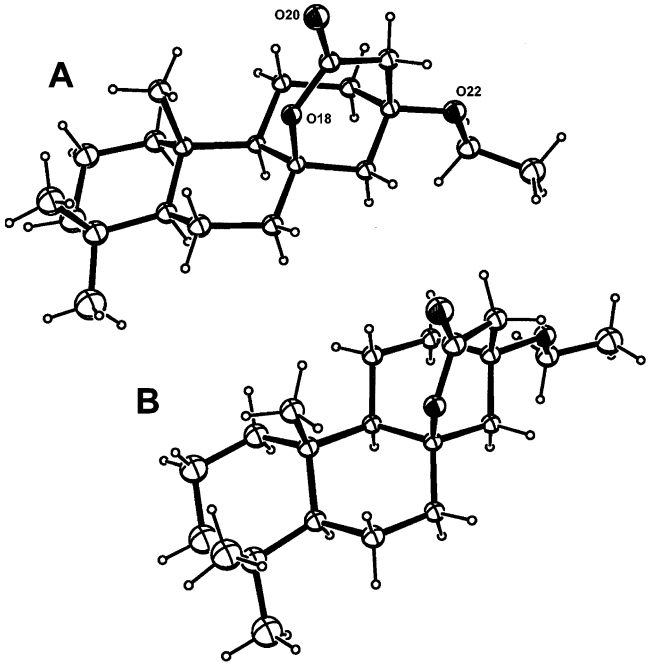

Figure 2. Perspective view of the two molecules of 17-norpimaran-13α-ethoxy-8,16-olactone (**8**) comprising the crystallographic asymmetric unit. Thermal ellipsoids for the non-hydrogen atoms are shown at the 50% probability level.

method afforded **6** and **7**, there was both a reduction in yield (32%) and a change in the *E*:*Z* ratio (2:1 as opposed to 4:3). On one occasion the lactone ether 17-norpimaran-13α-ethoxy-8,16-olactone (**8**) was isolated as a minor product (10%) from our one-pot synthesis. Crystallization of **8** from Et_2O/hexane and subsequent crystallographic analysis (Figure 2) provided both its structure and absolute configuration.[20] The two independent molecules A and B in the asymmetric unit adopt essentially the same conformation, except for the slightly different orientations of their ethyl groups. The fully assigned ^{1}H and ^{13}C NMR data for **8** are provided in Table 1, and a putative mechanism for the formation of **8** from **12** is presented in Scheme 1.

To increase the number of semisynthetic norditerpenoids available for antiplasmodial studies, we attempted to reduce the ester functionality in **6** with LAH to give the corresponding allylic alcohol. Surprisingly, LAH reduction of **6** gave exclusively the 1,4-Michael hydride addition product **9**, as evidenced by the disappearance of the olefinic resonances in both the ^{13}C and ^{1}H NMR spectra of **9** and the appearance of additional methylene (δ_C 40.4) and oxymethylene (δ_C 60.3) resonances in the DEPT135 NMR spectrum of this compound. The absence of duplicated resonances in the ^{13}C NMR spectrum of **9** suggested that the addition product was not epimeric at C-13. However, extensive overlap within the methylene envelope in the ^{1}H NMR spectrum of **9** in both deuterated chloroform and benzene prevented the assignment of the configuration at C-13. Interestingly, reduction of the *Z* isomer **7** yielded both the expected allylic alchol **10** and the hydride addition product **9**. The retention of the vinylic resonances [δ_C 123.5 (d) and 142.1 (s)], loss of the ester carbonyl resonance (δ_C 167.2), and the emergence of an additional oxymethylene resonance (δ_C 57.5) in the ^{13}C NMR spectrum of **10** unequivocally confirmed its structure.

Asili et al.[8] provided evidence to show that **1**−**4** and a number of unrelated labdane diterpenoids also caused echinocytic or stomatocytic changes to the erythrocyte membrane. Accordingly, they hypothesized that the weak or moderate antiplasmodial activity exhibited by nonpolar secondary metabolites was therefore not a sign of inhibitory activity against *P. falciparum* but rather an indirect effect arising from host cell membrane damage that occurs at

Table 1. ^{1}H (600 MHz) and ^{13}C (150 MHz) NMR Data of **8**

position	δ_C, mult	δ_H, mult (*J*)	HMBC	COSY
1	39.5	0.85, m	2, 10, 17	1b, 2a
		1.62, m	2	1a, 2a, 2b
2	18.4	1.39, m	1, 3, 4, 10	1a, 2b, 3a
		1.60, m		1a, 2a, 2b, 3b
3	41.9	1.12, m	2, 3, 18	2a, 2b, 3b
		1.40, m	1, 2, 4, 10	2b, 3a
4	33.2			
5	55.8	0.87, dd (12.2, 1.9)	6, 10	6
6	17.7	1.54, m	7	5, 7b
		1.70, m		
7	40.0	1.52, m	6, 8, 9, 13, 16	7b
		1.96, m	5, 6, 8, 13	6, 7a
8	83.0			
9	56.1	1.06, dd (12.5, 3.9)		11a, 11b
10	37.1			
11	18.6	1.20, m	10, 12	11b, 12a, 12b
		1.80, m	8, 9, 13	11a, 12a
12	35.6	1.57, m	13, 15	11a, 11b, 12b, 15a, 15b
		1.94, m	9, 13, 14	11a, 12b
13	71.6			
14	44.4	1.67, dd (12.8, 2.4)	8, 9, 13, 15	14b, 15a, 15b
		1.75, dd (12.8, 3.0)	8, 9, 13, 15	14a, 15a, 15b
15	41.1	2.58, dd (18.0, 1.8)	12, 13, 14, 16	12a, 15b
		2.66, dd (18.0, 2.3)	12, 13, 14, 16	
				14a, 15a
16	170.7			
17				
18	33.6	0.87, s	3, 4, 5, 19	
19	21.7	0.84, s	3, 4, 5, 19	
20	14.8	0.94, s	9, 10, 18	
1′	56.2	3.44, q (8.5)	2′, 13	2′
		3.45, q (7.0)	2′, 13	2′
2′	16.0	1.15, t (7.0)	1′	1′

Scheme 1 Putative mechanism for the Formation of 8 during the HWE Reaction

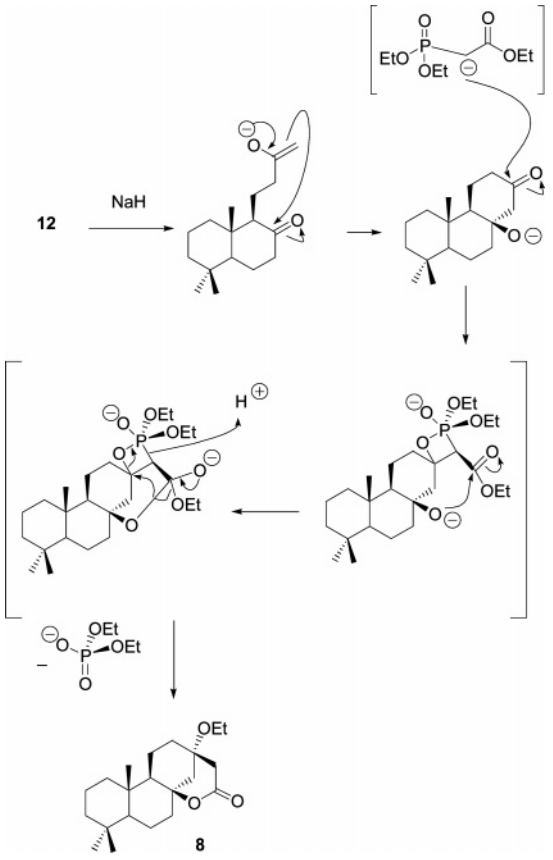

subhemolytic concentrations and is manifested by changes in the shapes of the erythrocytes. At least three of our semisynthetic compounds (**6**, **7**, **10**) show hemolytic activity in the 100−200 μg mL^{-1} range, measured as hemoglobin release into the culture medium (Table 2), suggesting that these compounds may accumulate in the erythrocyte membrane bilayer.[8] At 100 μg mL^{-1}, the most hemolytic compound (**10**) caused the majority of the erythrocytes to assume stomatocyte type III shapes and occasional erythrocyte ghosts were also present in the culture (Table 2, Figure 3G, H).[21] However, at lower concentrations erythrocytes retained their normal discocyte shape. The second most hemolytic compound (**7**) caused a mixture of knizocytes and type III stomatocytes in 17% of the erythrocytes at 100 μg mL^{-1} (Table 2, Figure 3D), while a small percentage of type II stomatocytes were formed by incubation with **6** (Figure 3C). Except for a modest increase in type I echinocytes found with **8** (Figure 3E; control cultures contain 3−4% type I echinocytes), the other compounds did not significantly affect erythrocyte shape at 100 μg mL^{-1} (Table 2, Figure 3). Compounds **6**, **7**, and **10**, which are the most hemolytic and "stomatocyte inducing", have the lowest IC_{50}'s, while **5**, **8**, and **9**, which have little or no hemolytic activity and do not cause stomatocyte formation in the concentration range tested, display the highest IC_{50}'s (Table 2). From the disparity between the IC_{50}'s and the concentrations at which shape changes and hemolysis occur we argue that erythrocyte shape changes *per se* may not be accountable for the parasite inhibitory activity of **5**, **8**, and **9** and allows for the possibility that these three compounds affect a parasite-specific intracellular target. However, the possibility does remain that the binding of **5**, **8**, and **9** to the erythrocyte membrane, at concentrations too low to cause erythrocyte shape changes or lysis, may remain sufficient to compromise erythrocyte function and hence parasite viability.

Experimental Section

General Experimental Procedures. Melting points were determined using a Reichert hot-stage microscope and are uncorrected. Optical rotations were measured using a Perkin-Elmer 141 polarimeter calibrated at the sodium D line (598 nm). IR spectra were recorded on a

Table 2. Parasite-Inhibitory and Hemolytic Properties of **5**−**10**

	5	**6**	**7**	**8**	**9**	**10**	CQ
IC_{50} (μg mL^{-1}) ± SD[a]	10.7 ± 5.3	5.7 ± 4.6	3.9 ± 1.2	19.6 ± 6.6	13.3 ± 5.1	10.6 ± 3.3	0.0103 ± 0.0023
% hemolysis[b] 200 μg mL^{-1}	0.2	17	34	0	5	102	ND
% hemolysis 100 μg mL^{-1}	0.6	3	9	0	0	2	ND
% stomatocytes[c] 100 μg mL^{-1}	1	8	17[d]	0	3	64	ND
% echinocytes 100 μg mL^{-1}	2	0	0	9	2	0	ND
% stomatocytes 50 μg mL^{-1}	1	2	11	1	1	5	ND
% echinocytes 50 μg mL^{-1}	3	2	0	2	3	1	ND

[a] Mean IC_{50} values and standard deviations (SD) were derived from IC_{50} determinations carried out on four separate occasions for **5**−**10** and on three occasions for chloroquine (CQ). [b] Percentage hemolysis was calculated relative to that obtained with 0.2% saponin. [c] The percentages of malformed erythrocytes (stomatocytes and echinocytes) present in erythrocyte samples incubated with the various compounds for 48 h are also indicated. Erythrocyte shapes were defined according to Lim et al.[21] ND = not determined. [d] Mixture of knizocytes and stomatocytes.

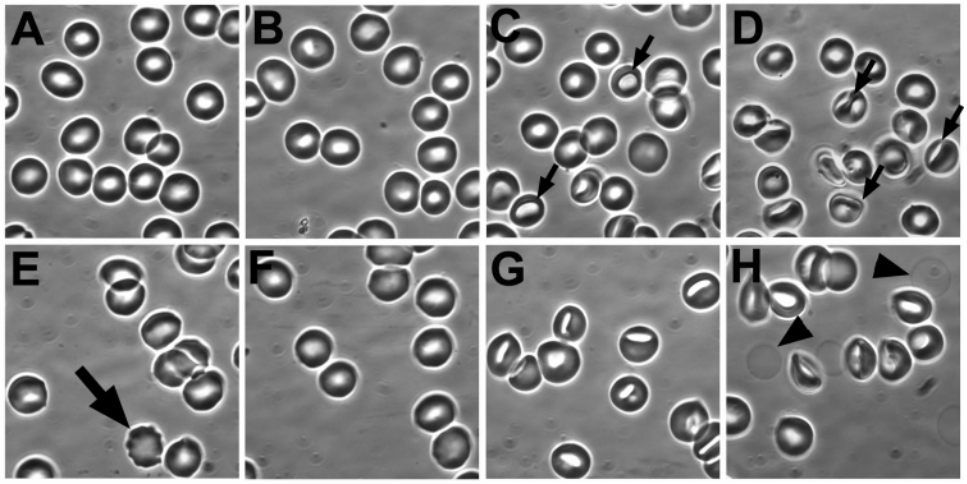

Figure 3. Phase-contrast micrograph of erythrocytes incubated with medium alone (A) or 100 μg mL^{-1} of compound **5** (B), **6** (C), **7** (D), **8** (E), **9** (F), and **10** (G, H). The erythocytes were mounted under coverslips and viewed directly by phase-contrast light microscopy. Small arrows indicate type II stomatocytes in C and knizocytes in D. Large arrow denotes a type I echinocyte in E, and arrowheads indicate erythrocyte ghosts in H.

Perkin-Elmer Spectrum 2000 FT-IR spectrometer with the compounds as films (neat) on NaCl discs. NMR spectra were acquired on Bruker 400 MHz Avance and 600 MHz Avance II spectrometers using standard pulse sequences. Chemical shifts are reported in ppm, referenced to residual solvent resonances ($CDCl_3$ δ_H 7.25, δ_C 77.2, C_6D_6 δ_H 7.15, δ_C 128.02), and coupling constants are reported in Hz. LREIMS (70 eV) and HRFABMS data were obtained on a Finnegan-Matt GCQ and a JEOL SX102 spectrometer, respectively. Kieselgel 60 (230−400 mesh) was used for initial flash chromatographic separations. Semipreparative HPLC was performed using a Whatman's Magnum 9 Partisil 10 column (10 mm i.d., length 50 cm) with an eluent flow rate of 4 mL min.$^{-1}$ Reactions where exclusion of water was necessary were performed in flame-dried glassware under Ar. Immediately prior to their use Et_2O and THF were distilled from sodium metal/benzophenone ketyl and CH_2Cl_2 was distilled from CaH_2. General laboratory solvents were distilled before use. Reactions were monitored by thin-layer chromatography (DC-Plastikfolien Kieselgel 60 F_{254} plates) and visualized under UV light and developed by spraying with either 10% concentrated H_2SO_4 in MeOH or I_2.

***(E)*- and *(Z)*-(5*S*,9*R*,10*S*)-Labda-8(17),13-dienal (14).** A solution of manool (**11**) (170 mg, 0.586 mmol) and pyridinium chlorochromate (417 mg, 1.93 mmol, 3.3 equiv) in CH_2Cl_2 (8 mL) was stirred (26 h) at room temperature. Et_2O (8 mL) was added, and the formation of an orange precipitate noted. The solution was then filtered through a Celite plug and the filtrate concentrated *in vacuo* to yield a dark brown oil (195 mg). The oil was purified on a silica column (EtOAc/hexane, 15:1) to yield a 2:1 inseparable mixture of the *E* and *Z* isomers of **14** (154 mg, 90% yield) as a pale yellow oil: ^{1}H and ^{13}C NMR data consistent with literature values;[22] HRFABMS *m*/*z* 289.2531 $[M + H]^+$ (calcd for $C_{20}H_{33}O$ 289.2531).

14,15,17-Trinorlabda-8,13-dione (12). The isomeric mixture of **14** (100 mg, 0.35 mmol) was dissolved in anhydrous CH_2Cl_2 (5 mL) and cooled to −78 °C. A steady stream of O_3 was bubbled through this solution (10 min) until the solution had turned a pale blue color, whereupon N_2 was bubbled through the solution to remove excess O_3. After the addition of triphenyl phosphine (548 mg, 2.09 mmol, 6 equiv) the solution was stirred at ambient temperature (4 h). The solution was cooled to 0 °C, H_2O_2 (30%, 1 mL) was added, and stirring continued (0.5 h). The solution was finally washed with H_2O (3 × 5 mL), and the combined organic extracts were dried (anhydrous $MgSO_4$) and concentrated. Subsequent purification of the concentrated organic material on a silica column (EtOAc/hexane, 1:1) afforded **12** (72.1 mg, 0.273 mmol, 78.4%): colorless oil; ^{1}H and ^{13}C NMR data consistent with literature values;[14,23,24] $[\alpha]_D^{20}$ −28.3 (*c* 1.3, $CHCl_3$), lit.[14] −11; IR ν_{max} 2940, 1709, 1698, 1355, 1164 cm^{-1}; HRFABMS *m*/*z* 265.2167 $[M + H]^+$ (calcd for $C_{17}H_{28}O_2$ 265.2168).

8-Hydroxy-13-podocarpanone (13). NaH (60%, 18.3 mg, 1 equiv) was added to a solution of **12** (241.2 mg, 0.913 mmol) in anhydrous THF (60 mL) and the resulting mixture stirred under Ar at ambient temperature (6 h). The yellow solution was concentrated to dryness, taken up in Et_2O (5 mL), and washed with H_2O acidified with a few drops of 1 M HCl (3 × 5 mL). The organic fraction was concentrated *in vacuo* to yield **13** (228 mg, 95%) as a pale yellow, amorphous mass: $[\alpha]_D^{28}$ +11.6 (*c* 2.2, $CHCl_3$); ^{1}H and ^{13}C NMR data consistent with literature values.[12]

17-Norisopimar-15-ene-8β,13β-diol (5). A THF solution of vinyl magnesium bromide (0.920 mmol, 1.5 equiv) was added to a cooled

(0 °C) solution of **13** (162.4 mg, 0.614 mol) in anhydrous THF under an Ar atmosphere. The solution was gradually warmed to ambient temperature and stirred (1.5 h). Et_2O (10 mL) and a saturated aqueous solution of NH_4Cl (6 mL) were added, and the resulting mixture was stirred for 10 min, after which the organic and aqueous phases were separated and the aqueous fraction was extracted with Et_2O (3 × 5 mL). The organic fractions were pooled, dried (anhydrous $MgSO_4$), and concentrated to yield a yellow oil (362 mg). This oil was subsequently purified by normal-phase HPLC (EtOAc/hexane, 3:1) to yield **5** as white crystals (from hexane): mp 157.5−159.5 (lit.[12] 154−155 °C); $[\alpha]_D^{28}$ −5.6 (*c* 2.6, $CHCl_3$); IR ν_{max} 3299, 2945, 1436, 1196, 761 cm^{-1}; ^1H NMR (C_6D_6, 600 MHz) δ 5.71 (1H, dd, J = 17.3, 10.7 Hz, H-15), 5.25 (1H, d, J = 13.7 Hz, H-16b), 4.96 (1H, d, 10.7 Hz, H-16a), 1.76 (1H, dq, J = 13.1, 3.2 Hz, H-11b), 1.63 (1H, m, H-7b), 1.60 (3H, m, H-1b, H-2b, H-12b), 1.59 (1H, m, H-6b), 1.52 (1H, dd, J = 14.0, 2.6 Hz, H-14b), 1.39 (1H, m, H-3b), 1.40 (1H, m, H-6a), 1.37 (2H, m, H-2a, H-11a), 1.21 (1H, dt, J = 13.7, 4.1 Hz, H-12a), 1.16 (1H, dd, J = 13.3, 3.9 Hz, H-3a), 1.13 (3H, s, H_3-20), 1.11 (1H, d, J = 14.0 Hz, H-14a), 1.04 (1H, ddd, J = 13.4, 12.9, 4.0 Hz, H-7a), 0.90 (3H, s, H_3-18), 0.89 (3H, s, H_3-19), 0.71 (2H, m, H-1a, H-5), 0.56 (1H, d, J = 12.6, 2.8 Hz, H-9) ppm; ^{13}C NMR data consistent with literature values;[12] LREIMS *m*/*z* (rel int) 293 [M^+] (1), 274 (72), 259 (100), 149 (39), 136 (45); HRFABMS *m*/*z* 293.2481 [M + H]$^+$ (calcd for $C_{19}H_{33}O_2$ 293.2480).

Ethyl 17-Norabiet-13(15)-*E*-en-8β-ol-16-oate (6) and Ethyl 17-Norabiet-13(15)-*Z*-en-8β-ol-16-oate (7). Triethyl phosphonoacetate (376 μL, 1.90 mmol, 2.5 equiv) was added to an anhydrous solution of NaH (60%, 38 mg, 1.90 mmol, 2.5 equiv) in THF (15 mL), and the mixture was stirred under an Ar atmosphere (0.5 h). A solution of **13** (264 mg, 0.761 mmol) in anhydrous THF (10 mL) was added via cannula and the reaction mixture stirred at ambient temperature (10 h), after which HCl (1 M, 3 drops) was added and the mixture concentrated *in vacuo*. The resulting oil was taken up in Et_2O (5 mL) and washed with H_2O (3 × 5 mL). The combined organic fraction was dried (anhydrous $MgSO_4$) and concentrated *in vacuo* to yield a yellow oil, which was subsequently purified on silica (EtOAc/hexane, 1:4) to yield a mixture of the *E*/*Z* isomers **6** and **7**. This mixture was further purified using normal-phase HPLC (EtOAc/hexane, 1:9) to yield **6** (105 mg, 41%) and **7** (76 mg, 29%). On one isolated occasion the minor product **8** was also isolated in 10% yield.

Compound 6: white crystals (from Et_2O); mp 110−111 °C; $[\alpha]_D^{34}$ −68.1 (*c* 1.8, $CHCl_3$); IR ν_{max} 2942, 1720, 1634, 1156, 1046 cm^{-1}; ^1H NMR ($CDCl_3$, 400 MHz) δ 5.60 (1H, t, J = 1.4 Hz, H-15), 4.13 (2H, q, J = 7.1 Hz, −OC*H*$_2$CH$_3$), 3.92 (1H, m, H-12b), 2.20 (1H, ddd, J = 13.1, 1.6, 0.7 Hz, H-14b), 2.05 (1H, dd, J = 13.1, 2.3 Hz, H-14a), 1.79 (1H, m, H-11b), 1.76 (1H, m, H-12a), 1.75 (1H, m, H-7b), 1.67 (1H, m, H-1b), 1.59 (1H, m, H-2b),1.58 (1H, m, H-6b), 1.44 (1H, m, H-7a), 1.43 (1H, m, H-11a), 1.40 (1H, m, H-6a), 1.39 (1H, m, H-3b), 1.38 (1H, m, H-2a), 1.26 (3H, t, J = 7.1 Hz, −OCH$_2$C*H*$_3$), 1.17 (1H, m, H-9), 1.14 (m, 1H, H-3a), 0.94 (3H, s, H_3-20), 0.87 (3H, s, H_3-18), 0.87 (1H, m, H-1a), 0.84 (3H, s, H_3-19) ppm; ^{13}C NMR ($CDCl_3$, 100 MHz) δ 166.3 (C, C-16), 159.4 (C, C-13), 116.1 (CH, C-15), 73.9 (C, C-8), 59.6 (CH_2, −O*C*H$_2$CH$_3$), 56.4 (CH, C-9), 56.3 (CH, C-5), 53.3 (CH_2, C-14), 42.1 (CH_2, C-3), 41.5 (CH_2, C-7), 39.7 (CH_2, C-1), 37.4 (C, C-10), 33.6 (CH_3, C-18), 33.3 (C, C-4), 29.6 (CH_2, C-12), 22.4 (CH_2, C-11), 21.7 (CH_3, C-19), 18.4 (CH_2, C-2), 18.3 (CH_2, C-6), 15.4 (CH_3, C-20), 14.3 (CH_3, −OCH$_2$*C*H$_3$) ppm; LREIMS *m*/*z* (rel int) 334 [M^+] (30), 319 (100), 273 (50), 207 (53), 149 (35); HRFABMS *m*/*z* 334.2509 [M]$^+$ (calcd for $C_{21}H_{34}O_3$ 334.2508).

Compound 7: yellow oil; $[\alpha]_D^{34}$ +66.3 (*c* 0.8, $CHCl_3$); IR ν_{max} 2941, 1695, 1652, 1165, 1037 cm^{-1}; ^1H NMR ($CDCl_3$, 400 MHz) δ 5.75 (1H, t, J = 1.5 Hz, H-15), 4.12 (2H, dq, J = 7.1, 1.0 Hz, −OC*H*$_2$-CH$_3$), 3.66 (1H, dd, J = 13.5, 0.9 Hz, H-14b), 2.34 (1H, m, H-12b), 2.11 (1H, dt, J = 12.8, 4.3 Hz, H-12a), 1.86 (1H, dd, J = 13.5, 0.9 Hz, H-14a), 1.78 (1H, m, H-11b), 1.77 (1H, m, H-7a), 1.67 (1H, m, H-1b), 1.62 (2H, m, H-2b, H-11a), 1.55 (1H, m, H-6b), 1.52 (1H, m, H-7a), 1.40 (1H, m, H-2a), 1.39 (1H, m, H-3b), 1.37 (1H, m, H-6a), 1.25 (3H, t, J = 7.1 Hz, −OCH$_2$C*H*$_3$), 1.16 (1H, m, H-9) 1.15 (1H, m, H-3a), 0.94 (3H, s, H_3-20), 0.88 (1H, m, H-5), 0.87 (3H, s, H_3-18), 0.86 (1H, m, H-1a), 0.84 (3H, s, H_3-19) ppm; ^{13}C NMR ($CDCl_3$, 100 MHz) δ 167.2 (C, C-16), 160.0 (C, C-13), 115.6 (CH, C-15), 74.3 (C, C-8), 59.7 (CH_2, −O*C*H$_2$CH$_3$), 56.7 (CH, C-9), 56.4 (CH, C-5), 45.3 (CH_2, C-14), 42.4 (CH_2, C-7), 42.1 (CH_2, C-3), 39.7 (CH_2, C-1), 37.9 (CH_2, C-12), 37.5 (C, C-10), 33.7 (CH_3, C-18), 33.3 (C, C-4), 23.5 (CH_2, C-11), 21.7 (CH_3, C-19), 18.5 (CH_2, C-2), 18.3 CH_2, C-6), 15.3 (CH_3, C-20), 14.3 (CH_3, −OCH$_2$*C*H$_3$) ppm; LREIMS *m*/*z* (rel int) 334 [M^+] (35), 319 (100), 273 (36), 255 (27), 207 (33); HRFABMS *m*/*z* 335.2582 [M + H]$^+$ (calcd for $C_{21}H_{35}O_3$ 335.2588).

Compound 8: needle-like crystals (from hexane); mp 143−144 °C; $[\alpha]_D^{25}$ +11.5 (*c* 0.7, $CHCl_3$); IR ν_{max} 2922, 2952, 1716, 1086, 986 cm^{-1}; ^1H and ^{13}C data, see Table 1; LREIMS *m*/*z* (rel int) 334 [M^+] (18), 319 (35), 288 (100), 276 (70), 228 (31); HRFABMS *m*/*z* 334.2509 [M]$^+$ (calcd for $C_{21}H_{34}O_3$ 334.2508).

General Procedure for the Preparation of 17-Norisopimarane-8β,15-diol (9) and 17-Norarabiet-13(15)-ene-8β,15-diol (10). A solution of either the ethyl ester **6** (90.4 mg, 0.272 mmol) or the ethyl ester **7** (59.1 mg, 0.180 mmol) in anhydrous THF (5 mL) was added to a cooled (0 °C) solution of LAH (2.2 equiv) in THF (5 mL). The solution was stirred (2.5 h) under Ar while gradually warming to ambient temperature. The remaining LAH was quenched with H_2O (2 mL), concentrated *in vacuo*, and taken up in Et_2O (5 mL), which was washed with H_2O (3 × 5 mL). The combined organic partition fractions were dried (anhydrous $MgSO_4$) and concentrated under reduced pressure to yield a yellow oil. The oil was purified by normal-phase HPLC (100% EtOAc). The reduction of the *Z* isomer **7** yielded saturated diol **9** (7.9 mg, 14.9%) and the allylic alcohol (**10**, 24.3 mg, 46.2%). The reduction of the *E* isomer **6** yielded exclusively **9** (34.7 mg, 43.3%).

Compound 9: yellow oil, $[\alpha]_D^{34}$ −9.8 (*c* 3.5, $CHCl_3$); IR ν_{max} 3361, 2921, 1451, 1060, 735 cm^{-1}; ^1H NMR (C_6D_6, 600 MHz) δ 3.43 (2H, t, J = 6.6 Hz, H_2-16), 1.72 (1H, m, H-12b), 1.70 (1H, m, H-13), 1.60 (1H, m, H-2b), 1.59 (2H, m, H-1b, H-2a), 1.51 (1H, m, H-7b), 1.44 (1H, m, H-11b), 1.43 (1H, m, H-6a), 1.42 (1H, m, H-11a), 1.39 (1H, m, H-3b), 1.36 (1H, m, H-6b), 1.33 (1H, m, H-14b), 1.27 (1H, m, H-15b), 1.25 (H-15a), 1.17 (1H, m, H-7a), 1.14 (1H, m, H-3a), 1.05 (3H, s, H_3-20), 0.90 (3H, s, H_3-18), 0.89 (3H, s, H_3-19), 0.72 (1H, m, H-5), 0.71 (1H, m, H-12a), 0.70 (1H, m, H-14a), 0.69 (1H, m, H-1a), 0.62 (1H, dd, J =12.4, 3.3 Hz, H-9) ppm; ^{13}C NMR ($CDCl_3$, 150 MHz) δ 71.3 (C, C-8), 60.3 (CH_2, C-16), 56.7 (CH, C-9), 56.5 (CH, C-5), 49.3 (CH_2, C-14), 42.8 (CH_2, C-7), 42.5 (CH_2, C-3), 40.4 (CH_2, C-15), 39.7 (CH_2, C-1), 37.5 (C, C-10), 33.88 (CH_2, C-12), 33.85 (CH_3, C-18), 33.5 (C, C-4), 29.4 (CH, C-13), 22.0 (CH_3, C-19), 20.7 (CH_2, C-6), 18.9 (CH_2, C-2), 18.5 (CH_2, C-11), 15.8 (CH_3, C-20) ppm; LREIMS *m*/*z* (rel int) 294 [M^+] (1), 279 (100), 261 (85), 243 (21), 179 (16); HRFABMS *m*/*z* 295.2637 [M + H]$^+$ (calcd for $C_{19}H_{35}O_2$ 295.2636).

Compound 10: yellow oil; $[\alpha]_D^{34}$ −10.8 (*c* 1.4, $CHCl_3$); IR ν_{max} 3446, 2945, 1709, 1386, 757 cm^{-1}; ^1H NMR ($CDCl_3$, 400 MHz) δ 5.65 (1H, dd, J = 8.1, 6.8 Hz, H-15), 4.12 (1H, dd, J = 11.6, 6.8 Hz, H-16b), 3.92 (1H, dd, J = 11.6, 8.1 Hz, H-16a), 2.49 (1H, dd, J = 13.2, 2.1 Hz, H-14b), 2.27 (1H, m, H-12b), 1.97 (1H, dt, J = 12.8, 4.5 Hz, H-12a), 1.79 (1H, m, H-7b), 1.77 (1H, m, H-14a), 1.72 (1H, m, H-11b), 1.64 (1H, m, H-1b), 1.58 (1H, m, H-2b), 1.54 (1H, m, H-6b), 1.45 (1H, m, H-7a), 1.40 (2H, m, H-3b, H-6a), 1.38 (1H, m, H-11a), 1.37 (1H, m, H-2a), 1.12 (1H, m, H-3a), 1.10 (1H, m, H-9), 0.94 (3H, s, H_3-20), 0.90 (1H, m, H-5), 0.87 (3H, s, H_3-18), 0.85 (1H, m, H-1a), 0.84 (3H, s, H_3-19) ppm; ^{13}C NMR ($CDCl_3$, 100 MHz) δ 142.1 (C, C-13), 123.5 (CH, C-15), 73.0 (C, C-8), 57.5 (CH_2, C-16), 56.7 (CH, C-9), 56.4 (CH, C-5), 44.4 (CH_2, C-14), 42.1 (CH_2, C-3), 41.3 (CH_2, C-7), 39.5 (CH_2, C-1), 37.4 (C, C-10), 36.7 (CH_2, C-12), 33.6 (CH_3, C-18), 33.3 (C, C-4), 23.1 (CH_2, C-11), 21.7 (CH_3, C-19), 18.4 (CH_2, C-6), 18.3 (CH_2, C-2), 15.4 (CH_3, C-20) ppm; LREIMS *m*/*z* (rel int) 292 [M^+] (2), 259 (86), 179 (92), 149 (100), 91 (93); HRFABMS *m*/*z* 293.2480 [M + H]$^+$ (calcd for $C_{19}H_{33}O_2$ 293.2481).

Malaria Parasite Viability, Hemolysis, and Erythrocyte Shape Assays. *P. falciparum* (3D7 strain) was cultured under an atmosphere of 3% CO_2, 4% O_2, and 93% N_2 in RPMI-1640 medium supplemented with 50 mM glucose, 0.65 mM hypoxanthine, 25 mM HEPES, 0.2% (w/v) $NaHCO_3$, 0.048 mg mL^{-1} gentamicin, 0.5% (w/v) Albumax II, and 2−4% (v/v) human O^+ erythrocytes. Parasite-infected erythrocytes from culture were mixed with fresh culture medium and erythrocytes to yield a 2% parasitemia and 2% hematocrit suspension and distributed in microtiter plates at 100 μL/well. Serial dilutions of each compound were prepared in a duplicate plate and transferred to the parasite plate at 100 μL/well. The plates were incubated at 37 °C for 48 h, and parasite viability in each well was determined by measuring parasite lactate dehydrogenase activity.[25] Parasite viabilities were determined relative to solvent controls (wells containing 0.5% DMSO). To assess hemolytic activity, duplicate plates containing normal, uninfected erythrocytes at 2% hematocrit were also incubated for 48 h with the various compound dilutions. The intact erythrocytes were sedimented in the microtiter plate wells by centrifugation at 200*g* for 3 min, and released hemoglobin

in the supernatants was measured by removing aliquots and measuring absorbance at 405 nm. Wells treated with 0.2% saponin (from Quillaja bark supplied by Sigma-Aldrich, Steinheim, Germany) were used as 100% hemolysis controls. Erythrocyte shape changes after 48 h incubation with the various test compounds were assessed by removing aliquots from treated wells and preparing Giemsa-stained thin blood smears for light microscopy. In addition, aliquots were wet-mounted under glass coverslips and viewed directly by phase-contrast microscopy. To assess the effects of the compounds on erythrocyte shape at subhemolytic concentrations, 2% hematocrit suspensions of fresh erythrocytes were incubated with parasite culture medium alone (control) or with medium containing 100, 50, or 25 μg mL^{-1} of the various compounds for 48 h. After incubation, the erythrocyte suspensions were mounted directly under coverslips on microscope slides and immediately viewed with a Nikon Eclipse E600 light microscope using a 100× Apochromat oil-immersion objective and phase contrast optics. Images were captured with a Media Cybernetics CoolSNAP-Pro monochrome cooled charge-coupled device camera. Discocytes, echinocytes, stomatocytes, and knizocytes in the samples were defined according to Lim et al.[21]

Acknowledgment. We would like to thank Professor B. Robinson of Westchem Industries, New Zealand, for the generous donation of manool. Financial assistance from the South African National Research Foundation (NRF), the Department of Environmental Affairs and Tourism, DAAD (Ph.D. bursary A.v.W), is gratefully acknowledged. Professor L. Fourie (North West University) is thanked for assistance with the acquisition of HRFABMS data. M.R.C. acknowledges research support from the University of Cape Town and the NRF.

Supporting Information Available: ^{1}H and ^{13}C NMR spectra of compounds **5**−**10**. This material is available free of charge via the Internet at http://pubs.acs.org.

References and Notes

(1) Snow, R. W.; Guerra, C. A.; Noor, A. M.; Myint, H. Y.; Hay, S. I. *Nature* **2005**, *434*, 214−217.
(2) Sachs, J.; Malaney, P. *Nature* **2002**, *415*, 680−685.
(3) Ridley, R. G. *Nature* **2002**, *415*, 686−693.
(4) Foley, M.; Tilley, L. *Pharmacol. Ther.* **1998**, *79*, 55−87.
(5) Mutabingwa, T. K. *Acta Trop.* **2005**, *95*, 305−315.
(6) Sams-Dodd, F. *Drug Discovery Today* **2005**, *10*, 139−147.
(7) Tagboto, S.; Townson, S. *Adv. Parasitol.* **2001**, *50*, 199−295.
(8) Asili, J.; Lambert, M.; Ziegler, H. L.; Staerk, D.; Sairafianpour, M.; Witt, M.; Asghari, G.; Ibrahimi, I. S.; Jaroszewski, J. W. *J. Nat. Prod.* **2004**, *67*, 631−637.
(9) Villamizar, J.; Plata, F.; Canudas, N.; Tropper, E.; Fuentes, J.; Orcajo, A. *Syn. Commun.* **2006**, *36*, 311−320.
(10) Vik, A.; Hedner, E.; Charnock, C.; Samuelsen, O.; Larsson, R.; Gundersen, L.-L.; Bohlin, L. *J. Nat. Prod.* **2006**, *69*, 381−386.
(11) Villamizar, J.; Fuentes, J.; Salazar, F.; Tropper, E.; Alonso, R. *J. Nat. Prod.* **2003**, *66*, 1623−1627.
(12) Buckwalter, B. L.; Burfitt, I. R.; Felkin, H.; Joly-Goudket, M.; Naemura, K.; Salomon, M. F.; Wenkert, E.; Wovkulich, P. M. *J. Am. Chem. Soc.* **1978**, *100*, 6445−6450.
(13) Wenkert, E.; Mahajan, J. R.; Nussim, M.; Schenker, F. *Can. J. Chem.* **1966**, *44*, 2575−2579.
(14) Do Khac Manh, D.; Fetizon, M.; Flament, J. P. *Tetrahedron* **1975**, *31*, 1897−1902.
(15) Sundararaman, P.; Herz, W. *J. Org. Chem.* **1977**, *42*, 813−819.
(16) For reviews of the HWE reaction see: (a) Maryanoff, B. E.; Reitz, A. B. *Chem. Rev.* **1989**, *89*, 863−927. (b) Boutagy, J.; Thomas, R. *Chem. Rev.* **1974**, *74*, 87−99.
(17) Kelly S. E. In *Alkene Synthesis. Comparative Organic Synthesis*; Trost, B. M., Ed.; Pergamon: Oxford, 1991; Vol. 1, pp 761−773.
(18) Manitto, P. In *Biosynthesis of Natural Products*; Sammes, P. G., Translation Ed.; Ellis Horwood Ltd.: Chichester, 1981; pp 257−260.
(19) X-ray analysis of **6**. Diffraction intensities were collected with Mo Kα radiation from a cubic fragment (0.10 × 0.11 × 0.12 mm^3) using ϕ- and ω-scans of 1.00° on a Nonius Kappa CCD diffractometer, with the crystal cooled to 113(2) K in a nitrogen stream. Crystal data for **6**: $C_{21}H_{34}O_3$, M = 334.48, orthorhombic, space group $P2_12_12_1$ (no. 19), a = 7.3750(2) Å, b = 9.7769(3) Å, c = 27.077(1) Å, V = 1952.4(1) Å^3, Z = 4, D_c = 1.138 Mg/m^3, μ(Mo Kα) = 0.074 mm^{-1}, F(000) = 736. A total of 4302 reflections were collected, of which 2405 were observed [$I > 2\sigma(I)$]. The structure was solved by direct methods and refined on F^2 using all data, with non-hydrogen atoms treated anisotropically. All H atoms were located and then added in idealized positions in a riding model. The final R factors were R_1 = 0.1455 (all data), 0.0510 (observed data), wR_2 = 0.0917 (all data), 0.0742 (observed data) for 222 parameters. Crystallographic data (excluding structure factors) have been deposited at the Cambridge Crystallographic Data Centre (deposition no. 620303).
(20) X-ray analysis of **8**. Diffraction intensities were collected with Mo Kα radiation from a specimen of dimensions 0.10 × 0.20 × 0.20 mm^3 using ϕ- and ω-scans of 1.00° on a Nonius Kappa CCD diffractometer, with the crystal cooled to 113(2) K in a nitrogen stream. Crystal data for **8**: $C_{21}H_{34}O_3$, M = 334.48, monoclinic, space group $P2_1$ (no. 4), a = 6.9880(1) Å, b = 22.0165(4) Å, c = 12.6710(3) Å, β = 101.345(1)°, V = 1911.36(6) Å^3, Z = 4, D_c = 1.162 Mg/m^3, μ(Mo Kα) = 0.075 mm^{-1}, F(000) = 736. A total of 8635 reflections were collected, of which 5846 were observed [$I > 2\sigma(I)$]. The structure was solved by direct methods and refined on F^2 using all data, with non-hydrogen atoms treated anisotropically. All H atoms were located and then added in idealized positions in a riding model. The final R factors were R_1 = 0.0828 (all data), 0.0387 (observed data), wR_2 = 0.0782 (all data), 0.0692 (observed data) for 441 parameters. Crystallographic data (excluding structure factors) have been deposited at the Cambridge Crystallographic Data Centre (deposition no. 620304).
(21) Lim, G. H. W.; Wortis, M.; Mukhopadhyay, R. *Proc. Natl. Acad. Sci. U.S.A.* **2002**, *99*, 16766−16769.
(22) Ravn, M. M.; Coates, R. M.; Flory, J. E.; Peters, R. J.; Croteau, R. *Org. Lett.* **2000**, *2*, 573−576.
(23) Bastard, J.; Duc, D. K.; Fetizon, M. *J. Nat. Prod.* **1984**, *47*, 592−599.
(24) Saragiotto, M. H.; Gower, A. E.; Marsaioli, A. J. *J. Chem. Soc., Perkin Trans. 1* **1989**, 559−562.
(25) Makler, M. T.; Hinrichs, D. J. *Am. J. Trop. Med. Hyg.* **1993**, *48*, 205−210.

NP0701071